XATOM: an integrated toolkit for X-ray and atomic physics

Sang-Kil Son[1] and Robin Santra[1,2]

[1]CFEL, DESY, Germany / [2]Department of Physics, University of Hamburg, Germany

Introduction

X-ray free-electron lasers (XFEL) open a new era in science and technology, offering many possibilities that have not been conceivable with conventional light sources. Because of their very high fluence within very short pulse duration, materials interacting with XFEL undergo significant radiation damage with ejection of electrons, leading to the creation of warm dense matter or plasma. To comprehend the underlying physics, it is crucial to understand detailed ionization and relaxation dynamics in individual atoms during XFEL pulses. Here we present an integrated toolkit to investigate X-ray–induced atomic processes and to simulate electronic damage dynamics. This toolkit can easily handle all possible electronic configurations of all atom/ion species, and calculate physical observables during/after intense X-ray pulses. It has been successfully applied to study many XFEL-related phenomena from multiphoton ionization to molecular imaging. The toolkit enables us to connect details of electronic dynamics in atoms and the evolution of atomic processes in plasmas generated by XFEL.

Diagrams of multiphoton absorption mechanisms in Ne induced by ultraintense X-ray pulses

Figure from Young *et al.*, *Nature* **466**, 56 (2010).

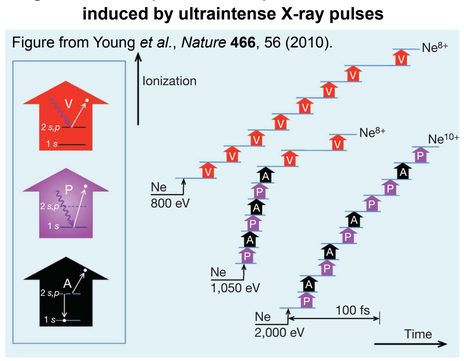

Theoretical and numerical details

Hartree-Fock-Slater model

To treat X-ray–atom interactions, we employ a consistent *ab initio* framework based on nonrelativistic quantum electrodynamics and perturbation theory. For implementation, we use the Hartree-Fock-Slater model, which employs a local density approximation to the exact exchange interaction, with the Latter tail correction.

$$\left[-\frac{1}{2}\nabla^2 + V(\mathbf{r})\right]\psi(\mathbf{r}) = \varepsilon\psi(\mathbf{r}), \text{ where } V(\mathbf{r}) = \begin{cases} -\dfrac{Z}{r} + \displaystyle\int \frac{\rho(\mathbf{r}')}{|\mathbf{r}-\mathbf{r}'|}\, d^3r' - \frac{3}{2}\left[\frac{3}{\pi}\rho(\mathbf{r})\right]^{1/3} \\ -\dfrac{Z - N_{\text{elec}} + 1}{r} \text{ for } r \to \infty \end{cases}$$

Rate equation model

To simulate electronic dynamics during intense X-ray pulses, we employ the rate equation approach with all computed cross sections and rates for all possible configurations, and calculate charge state distribution, electron and fluorescence spectra, scattering signals, and so on.

$$\frac{d}{dt}P_I(t) = \sum_{I' \neq I}^{\text{all config.}} \left[\Gamma_{I'\to I} P_{I'}(t) - \Gamma_{I\to I'} P_I(t)\right]$$

Towards plasmas

This toolkit is extendable to implement various plasma screening models that may cause atomic structural changes, and to include electron energy distributions and collisional ionization processes.

P **Photoabsorption**

$$\sigma_{\text{P}}(i,\omega) = \frac{4}{3}\alpha\pi^2\omega N_i \sum_{l_j=|l_i-1|}^{l_i+1} \frac{l_>}{2l_i+1}\left|\int_0^\infty P_{n_i l_i}(r) P_{\varepsilon l_j}(r)\, r\, dr\right|^2$$

F **Fluorescence**

$$\Gamma_{\text{F}}(i,j) = \frac{4}{3}\alpha^3 (I_i - I_j)^3 \frac{N_i^{\text{H}} N_j}{4l_j+2}\cdot\frac{l_>}{2l_i+1}\left|\int_0^\infty P_{n_i l_i}(r) P_{n_j l_j}(r)\, r\, dr\right|^2$$

A **Auger / Coster–Kronig decay**

$$\Gamma_{\text{A}}(i,jj') = \pi\frac{N_i^{\text{H}} N_{jj'}}{2l_i+1}\sum_{L=|l_j-l_{j'}|}^{l_j+l_{j'}}\sum_{S=0}^{1}\sum_{l_{i'}}(2L+1)(2S+1)|M_{LS}(j,j',i,i')|^2$$

Diagrams of X-ray–atom interaction

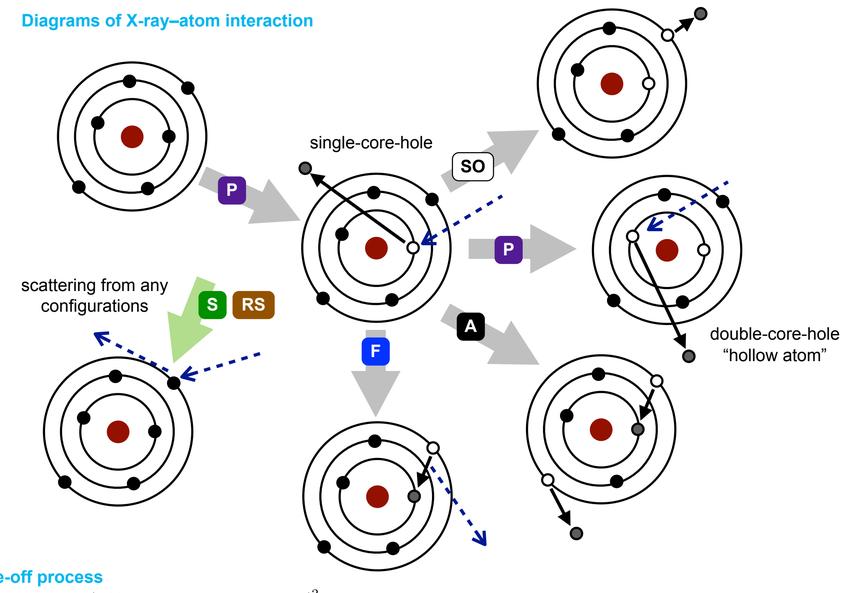

SO **Shake-off process**

$$p_{\text{SO}}(i;I,I') = 1 - \left|\int_0^\infty P_{n_i l_i}(r;I) P_{n_i l_i}(r;I')\, dr\right|^2$$

S **Coherent X-ray scattering**

$$f^0(\mathbf{Q}) = \int \rho(\mathbf{r})\, e^{i\mathbf{Q}\cdot\mathbf{r}}\, d^3r$$

$$\frac{d\sigma_{\text{S}}}{d\Omega}(t) = \sum_I^{\text{all config.}} P_I(t)\frac{d\sigma_{\text{S}}}{d\Omega}\Big|_I = \left(\frac{d\sigma}{d\Omega}\right)_{\text{T}} \sum_I^{\text{all config.}} P_I(t)|f_I^0(\mathbf{Q})|^2$$

RS **Resonant elastic X-ray scattering (dispersive correction)**

$$f(\mathbf{Q},\omega) = f^0(\mathbf{Q}) + f'(\omega) + if''(\omega)$$

$$f'(\omega) = -\frac{1}{2\pi^2\alpha}\mathcal{P}\int_0^\infty \frac{\omega'^2}{\omega'^2-\omega^2}\sigma_{\text{P}}(\omega')d\omega'$$

$$f''(\omega) = -\frac{\omega}{4\pi\alpha}\sigma_{\text{P}}(\omega)$$

C
scattering from hollow atom

$1s^2 2s^2 2p^2$
***N* of config. = 27**

One of the prospective applications of XFEL is single-shot imaging of individual macromolecules, which employs coherent X-ray scattering to determine the atomically resolved structure of non-crystallized biomolecules or other nanoparticles. During ultrashort and ultraintense X-ray pulses with an atomic scale wavelength, samples are subject to radiation damage, which may influence the quality of X-ray scattering patterns. Our numerical simulations of coherent X-ray scattering signals including electronic damage dynamics show that hollow-atom formation and the associated phenomenon of X-ray transparency or frustrated absorption play a crucial role in optimizing the strength and quality of single-shot X-ray scattering signals. The present results suggest that high-brightness attosecond XFELs would be ideal for single-shot imaging of individual macromolecules.

Normalized atomic form factor of carbon

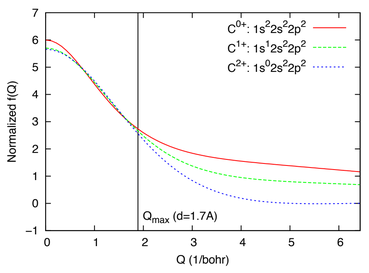

Number of scattered photons vs. fluence (8 keV and resolution=1.7 Å)

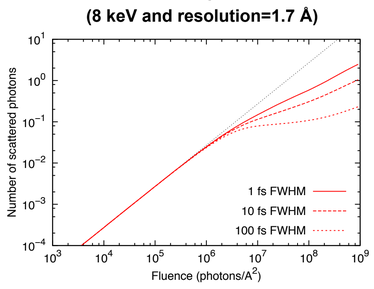

R-factor vs. resolution (10^7 photons/Å^2, 1 fs FWHM)

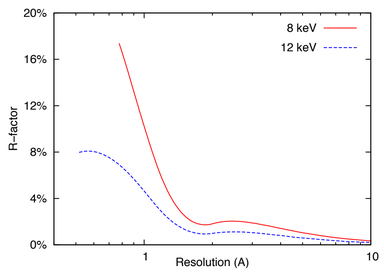

S.-K. Son, L. Young & R. Santra, *Phys. Rev. A* **83**, 033402 (2011)

Ne
nonlinear X-ray response

$1s^2 2s^2 2p^6$
***N* of config. = 63**

The study and applications of nonlinear processes from the micro-wave to the ultraviolet frequencies are extensive, but not realized for X-ray until now. We present the first experimental evidence of nonlinear response in the X-ray regime conducted at LCLS XFEL. In theory, we have extended our model to include shake-off processes and to adapt the two-photon ionization cross section for the rate equation model. We have measured and analyzed quadratic dependence of Ne^{9+} production on intensity when the photon energy is below the K-shell threshold of Ne^{8+}. Nonlinear response comes from two channels: direct two-photon ionization and sequential two-photon ionization with transient excited states competing with the Auger decay clock. This observation will boost the emergence of nonlinear X-ray physics.

Charge state distribution produced at 1110 eV (1.27 mJ)

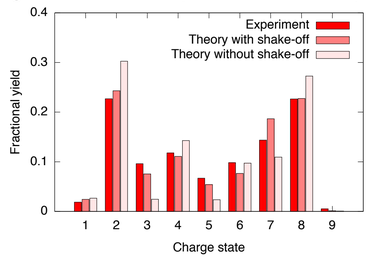

Two-photon ionization mechanisms at 1110 eV

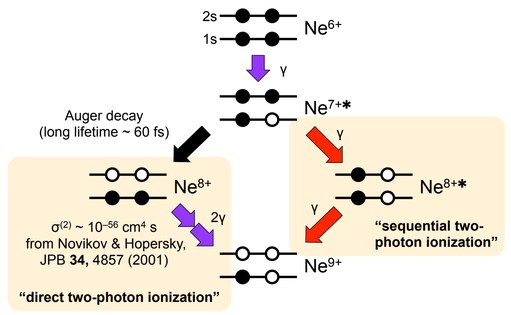

The Ne^{9+}/Ne^{8+} ratio as a function of X-ray pulse energy

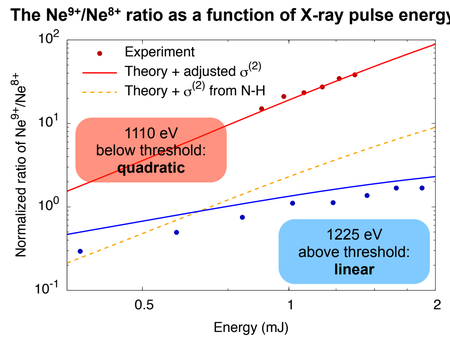

G. Doumy *et al.*, *Phys. Rev. Lett.* **106**, 083002 (2011)

Fe
MAD at high intensity

$1s^2 2s^2 2p^6 3s^2 3p^6 3d^6 4s^2$
***N* of config. = 27,783**

MAD (multi-wavelength anomalous diffraction) is used to determine phase information in X-ray crystallography by employing resonant elastic X-ray scattering from heavy atoms. We have recently proposed that the MAD phasing method can be extended to structural determination of molecules under intense X-ray pulses. The essential equation for the MAD method is reformulated and relevant coefficients are calculated with detailed electronic damage dynamics of heavy atoms and accompanying changes of the dispersion correction. Our study opens up a new opportunity of resolving the phase problem in femtosecond nanocrystallography with XFELs.

Dispersion corrections of several selected charge states of iron

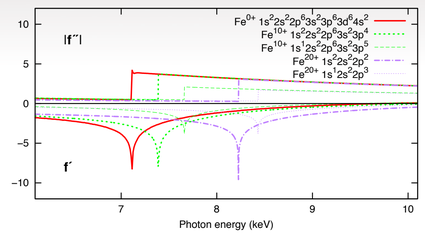

Generalized Karle-Hendrickson equation

$$\frac{dI(\mathbf{Q},\omega)}{d\Omega} = \mathcal{F}C(\Omega)\Big[\left|F_P^0(\mathbf{Q})\right|^2 + \left|F_H^0(\mathbf{Q})\right|^2 \tilde{a}(\mathbf{Q},\omega) + \left|F_P^0(\mathbf{Q})\right|\left|F_H^0(\mathbf{Q})\right| b(\mathbf{Q},\omega)\cos\left(\phi_P^0(\mathbf{Q}) - \phi_H^0(\mathbf{Q})\right) + \left|F_P^0(\mathbf{Q})\right|\left|F_H^0(\mathbf{Q})\right| c(\mathbf{Q},\omega)\sin\left(\phi_P^0(\mathbf{Q}) - \phi_H^0(\mathbf{Q})\right) + N_H\left|f_H^0(\mathbf{Q})\right|^2\{a(\mathbf{Q},\omega) - \tilde{a}(\mathbf{Q},\omega)\}\Big]$$

$$\tilde{a}(\mathbf{Q},\omega) = \frac{1}{\{f_H^0(\mathbf{Q})\}^2}\int_{-\infty}^{\infty} dt\, g(t)\left|\sum_{I_H} P_{I_H}(t) f_{I_H}(\mathbf{Q},\omega)\right|^2$$

$$a(\mathbf{Q},\omega) = \frac{1}{\{f_H^0(\mathbf{Q})\}^2}\sum_{I_H}\bar{P}_{I_H}\left|f_{I_H}(\mathbf{Q},\omega)\right|^2$$

$$b(\mathbf{Q},\omega) = \frac{2}{f_H^0(\mathbf{Q})}\sum_{I_H}\bar{P}_{I_H}\left\{f_{I_H}^0(\mathbf{Q}) + f'_{I_H}(\omega)\right\}$$

$$c(\mathbf{Q},\omega) = \frac{2}{f_H^0(\mathbf{Q})}\sum_{I_H}\bar{P}_{I_H} f''_{I_H}(\omega)$$

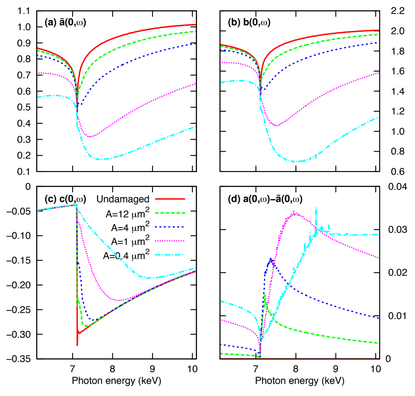

S.-K. Son, H. N. Chapman & R. Santra (submitted)

Xe
role of resonances

$1s^2 2s^2 2p^6 3s^2 3p^6 3d^{10} 4s^2 4p^6 4d^{10} 5s^2 5p^6$
***N* of config. = 1,120,581**

In recent experiments, the CFEL-MPG-ASG team has measured charge state distribution and fluorescence spectra of Xe atoms at LCLS XFEL. From theoretical point of view, this Xe problem is challenging because it has more than 1 million configurations and enormous numbers of processes are involved in electronic damage cascade. We have employed a Monte-Carlo approach to effectively solve the rate equation to attack this formidable task. Our numerical simulations show that charge state distribution of Xe is higher than expected from core-shell thresholds consideration, which can be explained by the multiple-core-hole states of 3*p* and 3*d* subshells in the intermediate charge states and resonantly enhanced absorption processes in the high charge states.

Time evolution of populations of several selected charge states of xenon in an XFEL pulse

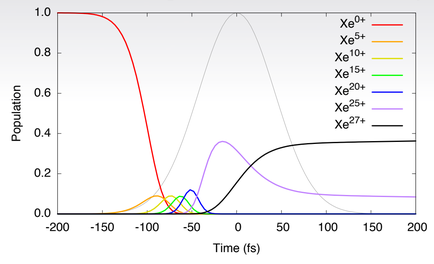

Charge state distribution of xenon (80 fs, 2.5 mJ, 3×3 μm²)

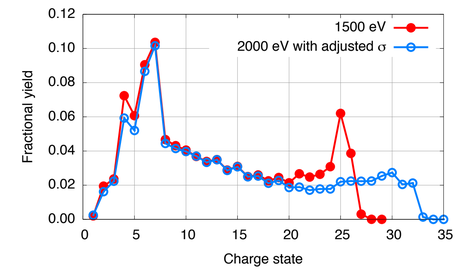

Fluorescence spectrum of xenon as a function of fluence

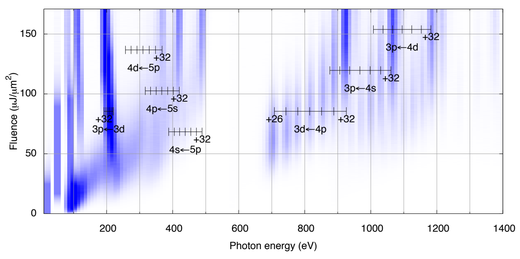

B. Rudek *et al.* (in preparation)
Collaboration with CFEL–MPG–ASG

Center for Free-Electron Laser Science

CFEL is a scientific cooperation of the three organizations:
DESY – Max Planck Society – University of Hamburg